


Systematic correlation analysis between the nuclear matter parameters and neutron star properties within relativistic mean-field theory

Shen Yang and Dehua Wen^{*}

*School of Physics and Optoelectronics, South China University of Technology,
Guangzhou 510641, People's Republic of China*

 (Received 25 September 2022; accepted 24 February 2023; published 10 March 2023)

Motivated by constraining the neutron star properties and eliminating their uncertainties based on the constraints on nuclear matter parameters extracted from the terrestrial experiments, the correlations between a mount of nuclear matter parameters and neutron star properties have been analyzed by the selected equation of states within the relativistic mean-field theory and used to constrain the neutron star properties. It is found that the radius R , tidal deformability Λ , and other neutron star properties have a notable correlation with the slope of symmetry energy L for the typical neutron stars, and the $R_{1.4}$ and $\Lambda_{1.4}$ restricted by the constraint on $L = 54 \pm 8$ MeV can be consistent with the GW170817 and NICER observation constraints. Furthermore, it is shown that L also has a good correlation with the properties of low-mass neutron stars, such as the gravitational binding energy $|E_g|$. The $|E_g|$ of low-mass neutron stars can be theoretically well constrained with the constraint range of L .

DOI: [10.1103/PhysRevD.107.063009](https://doi.org/10.1103/PhysRevD.107.063009)

I. INTRODUCTION

Neutron stars (NSs) are an ideal laboratory for the research of nuclear physics and astrophysics because of their environment of extreme high density, pressure, temperature, and magnetic fields, which cannot be reproduced in terrestrial laboratories at present [1]. In recent years, with the discovery of the gravitational wave event of binary NS merger (GW170817), the research on NSs has formally entered a new golden age [2–4]. At present, the theoretical research on NSs and their matter states is a research hotspot of NS physics and has received great attention. As we know, the properties of NS are significantly dependent on the equation of state (EOS), which is still obviously uncertain until now [5–9].

How to effectively constrain the properties of NSs is an important problem in NS physics. In addition to the general astronomical observations of NSs, another way is to use the data from the terrestrial nuclear experiments to constrain the NS properties. There are two effective methods to perform this research, i.e., the Bayesian analysis and correlation analysis [10–19]. At present, due to the development of experimental techniques, many valid constraints on the nuclear matter (NM) parameters can be extracted from the terrestrial experiments. For example, for the slope of symmetry energy at saturation density L , Oertel *et al.* gives a constraint $L = 58.7 \pm 28.1$ MeV based on a statistical analysis [7], and the recent PREX-2 experiment [20] gives

the new constraints on $L = 106 \pm 37$ MeV [21] or $L = 54 \pm 8$ MeV [22]. These experimental results provide us a valid way to restrict the NS properties, such as the radius R and tidal deformability Λ [12–17,23–31]. Moreover, based on the constraints of NS properties from the NM parameters, we can further explore the relations between the nuclear physics and NS astronomical observation [6,7,18].

In this work, we are mainly concerned with the correlation analysis between the NM parameters and NS properties. There are many important correlations between the NM parameters and NS properties, such as the correlation between the radius $R_{1.4}$ and L , which has been confirmed by many previous works [11,13,18,27,32–34]. For example, Malik *et al.* systematically studied the correlations between the NM parameters and NS properties, including the correlations of single NM parameter or the linear combination of two NM parameters [13,18,33,34]. Further, they applied the obtained correlations to constrain the NS properties, such as the $R_{1.4}$ and $\Lambda_{1.4}$. Their results can be in good agreement with the results of GW170817 and other previous works [4,12,35]. However, there are still many topics worth further exploration on this issue. For example, (1) some other NS properties are worth considering, such as the compactness β and the binding energy E_b [36–38], (2) the extended linear combinations, such as the linear or nonlinear combinations of more NM parameters, deserve further consideration.

In this work, we will use the relativistic mean-field (RMF) theory [39,40] to analyze the correlations between the NM parameters and NS properties, and further apply the correlations. First, similar to the previous works, we

^{*}Corresponding author.
wendehua@scut.edu.cn

will study the basic correlations between the NM parameters and NS properties, including the correlations of single NM parameter and a linear combination of two NM parameters, and apply these correlations. Further, we will extend the correlations to the case of the linear or nonlinear combinations of more NM parameters. Also, in addition to studying the correlations of the typical NSs, such as the $1.4M_{\odot}$ NSs, we will also concern the correlations between the properties of low-mass NSs and the NM parameters [41–43]. At last, using the constraints on the NS properties from the NM correlations, we will try to explore the relations between the NM parameters and the astronomical observations of NSs.

The paper is organized as follows. The theoretical framework are briefly reviewed in Sec. II, specifically including the NM parameters at saturation density in Sec. II A, and the EOS selection based on the RMF theory and the corresponding mass-radius relation of NSs in Sec. II B. The correlations between the NM parameters and NS properties and its application will be discussed in Sec. III, where the basic correlation analysis between the NM parameters and NS properties is presented in Sec. III A, and the extended correlation analysis between the NM parameters and NS properties is presented in Sec. III B. Finally, a brief summary is given in Sec. IV. In this work, we use the geometric units ($G = c = 1$).

II. THEORETICAL FRAMEWORK

In this section, we will briefly introduce the theoretical framework by two parts: (1) the NM parameters at saturation density; (2) the EOS selection based on the RMF theory and the corresponding mass-radius relation of NSs.

A. The nuclear matter parameters at saturation density

In uniform NM, the energy per nucleon $e(\rho, \delta)$ can be generally decomposed into two parts according to its parabolic type,

$$e(\rho, \delta) = e(\rho) + S(\rho)\delta^2, \quad (2.1)$$

where $e(\rho)$ is the symmetric NM part (isospin scalar), $S(\rho)\delta^2$ is the symmetry energy part (isospin vector), $\rho = \rho_n + \rho_p$ is the baryon density, $\delta = (\rho_n - \rho_p)/\rho$ is the isospin asymmetry, ρ_n and ρ_p are the density of neutron and proton, respectively. The above two parts can be further expanded to the third term and the second term, respectively, at the nuclear saturation density ρ_0 as

$$e(\rho) = e_0(\rho_0) + \frac{K_0}{2}x^2 + \frac{J_0}{6}x^3 + O(x^4), \quad (2.2)$$

$$S(\rho) = E_{\text{sym}}(\rho_0) + Lx + \frac{K_{\text{sym}}}{2}x^2 + O(x^3), \quad (2.3)$$

where $x = \frac{\rho - \rho_0}{3\rho_0}$, e_0 , K_0 , J_0 are the energy, incompressibility and skewness coefficient of symmetric NM at the saturation density respectively; $E_{\text{sym}}(\rho_0)$ is the symmetry energy at saturation density, which can be defined as the second derivative of $e(\rho, \delta)$ with respect to δ ; L and K_{sym} are the density slope and curvature of symmetry energy, respectively [13,16]. We can also define the slope of the incompressibility M_0 at saturation density as [11,13,44]

$$M_0 = 12K_0 + J_0. \quad (2.4)$$

Among the above various NM parameters, due to the restrictions of the terrestrial nuclear experiments, ρ_0 , e_0 , E_{sym} can be measured accurately now, and their uncertainty range is small; for other NM parameters, such as K_0 , J_0 , M_0 , L , K_{sym} , the experimental constraints on these quantities are still not obvious at present, and their uncertainty range is large.

B. The EOS selection based on the RMF theory and mass-radius relation of neutron stars

In this work, we will use two kinds of RMF theory for the study of the correlations between the NM parameters and NS properties, i.e., the nonlinear relativistic mean-field (NLRMF) and the density-dependent relativistic mean-field (DDRMF) models [39,40]. Both the NLRMF and DDRMF models will be used to describe the homogeneous neutron, proton, electron and muon (n, p, e, μ) matter of the NS core in β -equilibrium at zero temperature. Specifically, we selected 22 sets of RMF-EOS in this research, including: (1) 5 consistent relativistic mean-field (CRMF) EOSs finally selected by Lourenço *et al.* through a series works [26,40,45], i.e., G2* [46], IU-FSU [47], DD-F [48], TW99 [49], DD-ME δ [50]; (2) 17 DDRMF and NLRMF EOSs, i.e., DD-ME1 [51], DD-ME2 [52], PKDD [53], DD-LZ1 [54], DD [55], DD2 [56], NL1 [57], NL2 [57], NLZ [58], NLZ2 [58], NL3* [59], NL-SH [60], TM1 [61], PK1 [53], PK1R [53], NLSV1 [62], NLSV2 [62]. The above 22 selected EOSs can be able to cover a relatively large parameter space of NM, such as $K_0 = 170\text{--}400$ MeV for the incompressibility and $L = 40\text{--}145$ MeV for the density slope of symmetry energy at saturation density, which is convenient for the statistical analysis.

The above 22 selected RMF-EOSs will be used as the core-EOS of NSs, for the crust region at low density, we choose the BPS + BBP models as the outer and inner crust-EOSs respectively [63,64]. For the matching of the core and crust EOSs, we adopt the linear matching method given in Ref. [65]. The matching density is selected as 0.08 fm^{-3} for the core-EOS, at which the deviation between the NS properties obtained by the matched EOS and the unified EOS will reach the minimum [66]. With the above matching procedure of core-crust EOS, we can construct the complete BPS + BBP + RMF-matched EOS for NSs.

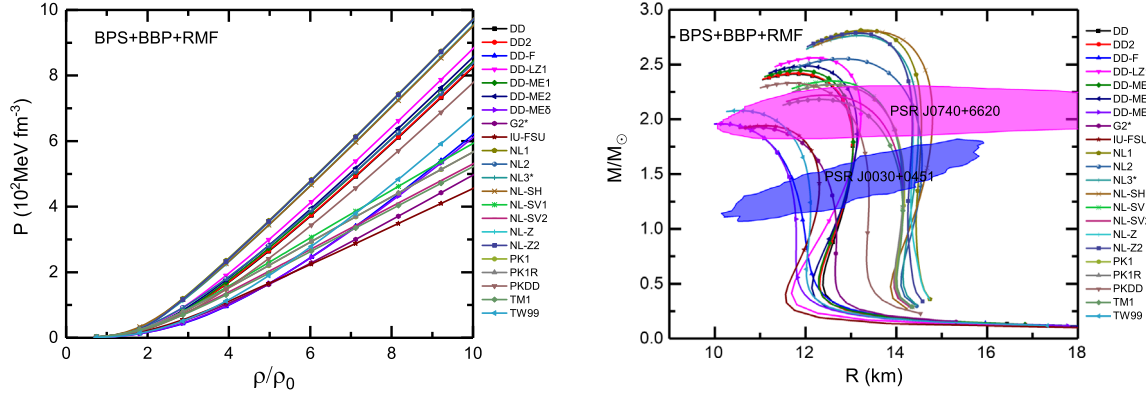


FIG. 1. Left panel: the pressure P of NSs as functions of the baryonic density in unit ρ/ρ_0 , where ρ_0 means the nuclear saturation density; right panel: the corresponding M - R relation of NSs. All of the results are given by the 22 selected BPS + BBP + RMF-matched EOSs. In the right panel, the blue and magenta areas represent the constraints from the NICER observations PSR J0030 + 0451 [69,70] and PSR J0740 + 6620 [71,72] with 95% credibility level, respectively.

Taking the EOS of NSs into the Tolman-Oppenheimer-Volkov (TOV) equations [67,68], we can get the mass-radius (M - R) relations. The left and right panels of Fig. 1 show the curves of P - ρ and M - R relations of NSs described by the selected 22 BPS + BBP + RMF-matched EOSs, respectively. Also, for verifying the rationality of the selected EOSs, we have added the recent astronomical observational constraints on NSs in the right panel, which are shown by different color areas, i.e., the M - R constraints from the NICER observations PSR J0030 + 0451 [69,70] and PSR J0740 + 6620 [71,72] with 95% credibility level, respectively. It is shown that the curves of M - R relations given by all of the 22 selected EOSs can be in good agreement with the recent astronomical observation constraints on NSs.

III. RESULTS AND DISCUSSIONS

In this section, we will use the selected 22 matched EOSs mentioned in Sec. II to discuss the correlations between the NM parameters and NS properties and their application. We adopt the linear correlation analysis method to study these correlations [16,34,38]. The linear correlation coefficient r , which can effectively reflects the strength of linear correlation between two quantities, can be expressed as

$$r(X, Y) = \frac{\text{Cov}(X, Y)}{\sqrt{D(X)}\sqrt{D(Y)}}, \quad (3.1)$$

where X, Y represent the object variables, $\text{Cov}(X, Y)$ is the covariance, and $D(X), D(Y)$ represent the variance of X, Y respectively [16,34,38]. The closer the correlation coefficient $|r|$ is to 1, the greater the correlation strength between the two quantities will be and the closer it is to linearity; conversely, the closer $|r|$ is to 0, the smaller the correlation strength will be.

In the following parts, we will focus on the correlations between the different NM parameters and the NS properties.

For the properties of NSs, we mainly concern the following quantities: (1) the radius R , the central density ρ_c and pressure P_c ; (2) some dimensionless quantities, including the dimensionless tidal deformability Λ , the dimensionless compactness parameter β , the moment of inertia I and the gravitational redshift z ; (3) the binding energy of NSs, which can be divided into three forms: the total binding energy E_t , the gravitational binding energy E_g and the nuclear binding energy E_n . For further details to the definition of the above quantities, please refer to Refs. [36–38]. Finally, after obtaining some valuable correlations, we will try to use these correlations to constrain the NS properties and then compare them with the NS astronomical observations to find some key information that affects the NS properties.

A. The basic correlation analysis between the NM parameters and NS properties

In this subsection, we will mainly analyze the basic correlations between the NM parameters and NS global properties similar to the previous works [11,13,18,33,34], and further try to use the obtained correlations to constrain the NS properties, and compare them with the astronomical observations. Specifically, we will analyze the correlations between the single NM parameter or the linear combinations of two NM parameters and the global properties of NSs. The correlation of the linear combination of multiple NM parameters are introduced mainly to find a better correlation than that of the single NM parameter.

Figure 2 shows the linear correlation coefficients $r(X, Y)$ between the NM parameters and several NS properties at fixed masses as functions of the NS mass in the typical mass range of NSs ($0.4 - 2.2M_\odot$). It can be seen that the correlations between different NM parameters and NS properties show the obvious different behaviors. In the whole mass range, the quantities which have a good correlation with R, Λ, β, E_n mainly are E_{sym} and L . Their correlation coefficients r are almost greater than

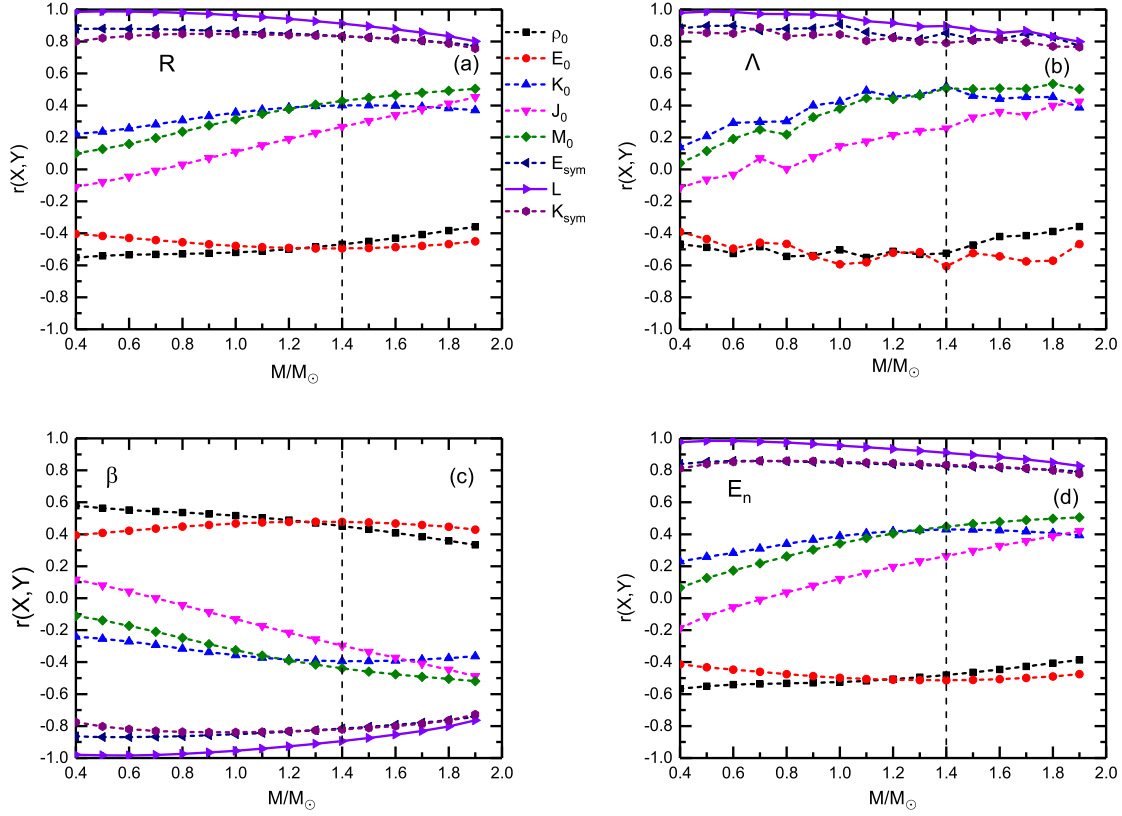


FIG. 2. The linear correlation coefficients $r(X, Y)$ between the different NM parameters and the NS properties at fixed mass as functions of the NS mass $M(M_\odot)$ by the selected 22 matched EOSs. The vertical black dashed line represents the position of $1.4M_\odot$. Plot (a): correlations with the radius R ; plot (b): correlations with the dimensionless tidal deformability Λ ; plot (c): correlations with the dimensionless compactness parameter β ; plot (d): correlations with the nuclear binding energy E_n .

0.9. Since the symmetry energy E_{sym} at ρ_0 has been well constrained in a small range (30–35 MeV) at present [9], it is unnecessary to consider it in the current analysis. Therefore, we can confirm that in the whole mass range of NSs, the NM parameter that has a good correlation with the NS properties is the slope of symmetry energy L , which is consistent with the previous conclusions [11,13,18,32]. Using the correlation of L , and combining with the constraints on L from the terrestrial experiments, we can constrain some NS properties and further compare them with the astronomical observations.

Figure 3 shows the results of correlation of $R_{1.4}$ ($\Lambda_{1.4}$) to the slope of symmetry energy L for $1.4M_\odot$ NSs. It is shown that $R_{1.4}$ ($\Lambda_{1.4}$) have a good linear correlation with L , and their linear correlation coefficients r are 0.912 (0.897), respectively. Similarly, $\beta_{1.4}$ ($E_{n,1.4}$) are also well correlated to L with $r = -0.894$ (0.910), respectively, which are not shown in the figure. The above four correlations can be simply expressed as,

$$R_{1.4} = 0.025L + 11.173, \quad (3.2)$$

$$\Lambda_{1.4} = 9.522L + 47.630, \quad (3.3)$$

$$\beta_{1.4} = -2.956 \times 10^{-4}L + 0.181, \quad (3.4)$$

$$E_{n,1.4} = 1.585 \times 10^{-4}L + 0.027. \quad (3.5)$$

Next, we studied the correlations between the linear combinations of two NM parameters and NS properties. Similar to the previous works [11,13,18,34], in this work, we will concern some common combinations of two NM parameters, such as $K_0 + aL$, $M_0 + aL$, and $K_0 + aK_{\text{sym}}$ etc. It is found that $M_0 + aL$ has the best correlation with the NS properties among these NM parameter combinations. We only show the correlations of $M_0 + aL$, such as the $(M_0 + aL)$ - $R_{1.4}$ ($\Lambda_{1.4}$), which are shown in Fig. 4. It is shown that when coefficient a respectively takes 73.5 (55.5), $(M_0 + aL)$ - $R_{1.4}$ ($\Lambda_{1.4}$) will take the maximum correlation values, the coefficients r are 0.958 (0.972) respectively. Similar to the analysis in Fig. 3, the $\beta_{1.4}$ ($E_{n,1.4}$) are also well correlated to $M_0 + aL$ with $r = -0.945$ (0.962) when $a = 68.0$, respectively. It is found that the correlations of $M_0 + aL$ are better than the correlations of L in Fig. 3. This illustrates that the linear combinations of NM parameters can also be used to

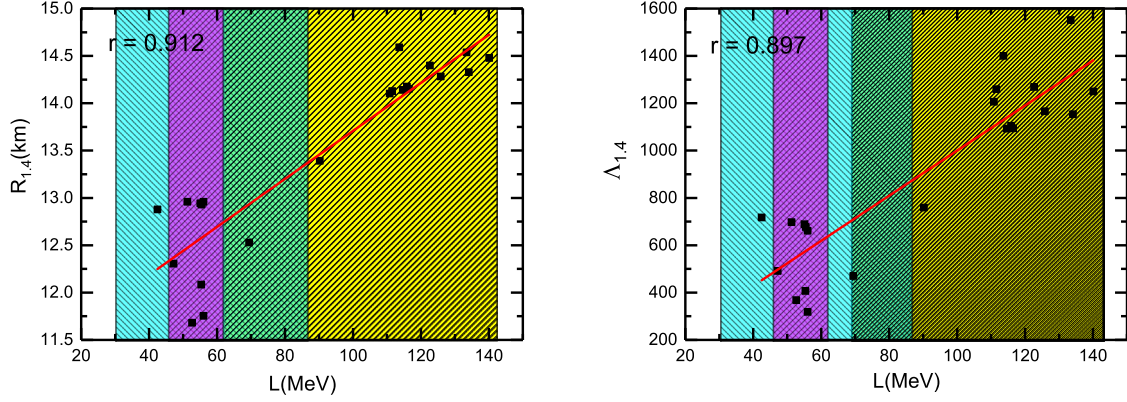


FIG. 3. The correlations between the slope of symmetry energy L and the NS properties at $1.4M_{\odot}$ given by the selected 22 matched EOSs. The yellow, magenta, and cyan shaded areas in each panel represent the constraints on $L = 106 \pm 37$ MeV [21] and $L = 54 \pm 8$ MeV [22] from PREX-2 experiment, and $L = 58.7 \pm 28.1$ MeV from Ref. [7], respectively. Each point in every panel represents the result given by one of the 22 selected EOSs. Left panel: correlations with the radius $R_{1,4}$; right panel: correlations with the dimensionless tidal deformability $\Lambda_{1,4}$.

constrain the NS properties according to its correlations. The above four correlations with $M_0 + aL$ can be expressed as,

$$R_{1,4} = 3.280 \times 10^{-4}(M_0 + 73.5L) + 10.302, \quad (3.6)$$

$$\Lambda_{1,4} = 0.161(M_0 + 55.5L) - 379.102, \quad (3.7)$$

$$\beta_{1,4} = -4.116 \times 10^{-6}(M_0 + 68.0L) + 0.192, \quad (3.8)$$

$$E_{n,1,4} = 2.207 \times 10^{-6}(M_0 + 68.0L) + 0.021. \quad (3.9)$$

Using Eqs. (3.2)–(3.5) and (3.6)–(3.9), the relative quantities of $1.4M_{\odot}$ NSs can be constrained according to the nuclear experiment constraints on L and M_0 (for example, $M_0 = 1800$ – 2400 MeV [44]). Alternatively, the NM parameters can be constrained based on the accurately astronomical observations of NSs.

Table I shows the constraints on the NS properties based on the correlations and constraint ranges of L and

$M_0 + aL$. For the constraints on L , we adopt three specific constraints in this work, i.e., $L_1 = 58.7 \pm 28.1$ MeV by Oertel *et al.* [7], $L_2 = 106 \pm 37$ MeV [21], and $L_3 = 54 \pm 8$ MeV [22] from the recent PREX-2 experiment [20]. In Table I, it is shown that the correlations of $M_0 + aL$ with the NS properties are better than the correlations of L . Furthermore, it is also found that compared with the results of L_1 and L_2 , the constraint ranges of $R_{1,4}$ and $\Lambda_{1,4}$ given by L_3 , especially for the results of $M_0 + aL_3$, i.e., $R_{1,4} = 12.00$ – 12.58 km, $\Lambda_{1,4} = 321.7$ – 561.3 , are more consistent with the constraints of GW170817 ($R_{1,4} < 13.5$ km, $\Lambda = 190^{+390}_{-120}$), NICER PSR J0030 + 0451 and others works [4,11,13–15,19,35,69,70]. The results indicate that compared with other constraints on L , the constraint on $L = 54 \pm 8$ MeV can give the more consistent results of NS properties with the existing astronomical observation constraints.

In summary, based on our selected 22 BPS+BBP+RMF-matched EOSs, similar to the previous works [11,13,18,33,34], we analyzed in detail the basic

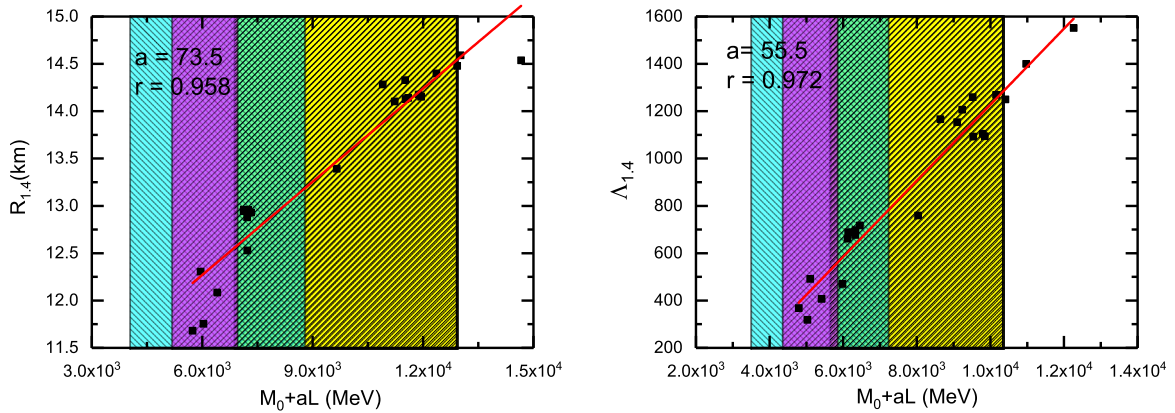


FIG. 4. Same as Fig. 3, but for the results of the NM parameter combination $M_0 + aL$, where a is the combination coefficient.

TABLE I. The NS properties at $M = 1.4M_\odot$, i.e., the radius $R_{1.4}$ (km), dimensionless tidal deformability $\Lambda_{1.4}$, compactness $\beta_{1.4}$, and nuclear binding energy $E_{n,1.4}$ (M_\odot), constrained by the correlations with L or $M_0 + aL$ (a represents the coefficient when the correlation is maximized). r represents the linear correlation coefficient, and L_1, L_2, L_3 represent the constraints $L_1 = 58.7 \pm 28.1$ MeV [7], $L_2 = 106 \pm 37$ MeV [21], $L_3 = 54 \pm 8$ MeV [22], respectively.

	L				$M_0 + aL$				
	r	L_1	L_2	L_3	a	r	L_1	L_2	L_3
$R_{1.4}$	0.912	11.95–13.38	12.93–14.81	12.34–12.75	73.5	0.958	11.63–13.18	12.56–14.54	12.00–12.58
$\Lambda_{1.4}$	0.897	339.0–874.1	704.7–1409.3	485.6–638.0	55.5	0.972	182.1–782.9	527.3–1285.1	321.7–561.3
$\beta_{1.4}$	-0.894	0.155–0.172	0.139–0.161	0.163–0.167	68.0	-0.945	0.158–0.176	0.142–0.165	0.165–0.172
$E_{n,1.4}$	0.910	0.032–0.041	0.038–0.050	0.034–0.037	68.0	0.962	0.030–0.039	0.035–0.048	0.032–0.036

correlations between the NM parameters and the global NS properties, including the cases of a single NM parameter and the linear combination of two NM parameters. We got some valuable correlations, such as the L - $R_{1.4}$ and L - $\Lambda_{1.4}$, which can be used to restrict the NS properties based on the constraint on L . The results show that compared with the results given by the other two constraints on $L = 58.7 \pm 28.1$ MeV [7] and $L = 106 \pm 37$ MeV [21], the results of $R_{1.4}$ and $\Lambda_{1.4}$ given by the constraint on $L_3 = 54 \pm 8$ MeV [22] are more consistent with the constraints of GW170817 and other previous works. It is shown that the core-crust EOS matching has a certain effect on the numerical results of the NS properties and their correlations with the NM parameters, but has little effect on the final qualitative conclusions. Compare the results given by the three constraints on L , in the following sections, we will use the constraint on $L = 54 \pm 8$ MeV to restrict the NS properties.

B. Extended correlation analysis between the NM parameters and NS properties

In Sec. III A, we mainly analyze the basic correlations between the NM parameters and the NS properties, and our research object is mainly the typical NSs, such as the

$1.4M_\odot$ NSs. In this subsection, we will extend the above research. Specifically, we will focus on the impact of the linear combinations of three NM parameters on the correlation. And besides the typical neutron stars, we will also concern ourselves with the correlations of the low-mass NSs ($M \leq 1.0M_\odot$).

Figure 5 shows the behavior of correlations between the linear combination of three NM parameters $K_0 + aL + bK_{\text{sym}}$ and $R_{1.4}$ ($\Lambda_{1.4}$) as they vary with the combination coefficients a, b . As shown in Fig. 5, when the correlation coefficients r take the maximum value, the value of the coefficient b is very small and almost negligible. Correspondingly, as the value of bK_{sym} is very small, its impact on the correlation can almost be ignored. Therefore, for the correlation of $K_0 + aL + bK_{\text{sym}}$, it is enough to focus on the first two items $K_0 + aL$. Similarly, Fig. 6 also shows the correlations between the linear combination of three NM parameters $M_0 + aL + bK_{\text{sym}}$ and $R_{1.4}$ ($\Lambda_{1.4}$), the results are also the same as those of Fig. 5. That is to say, when analyzing the correlation between the linear combination of NM parameters and the NS properties, generally it is enough to consider the first two items of the linear combination, there is no need to further consider the impact of the third or more items on the correlation.

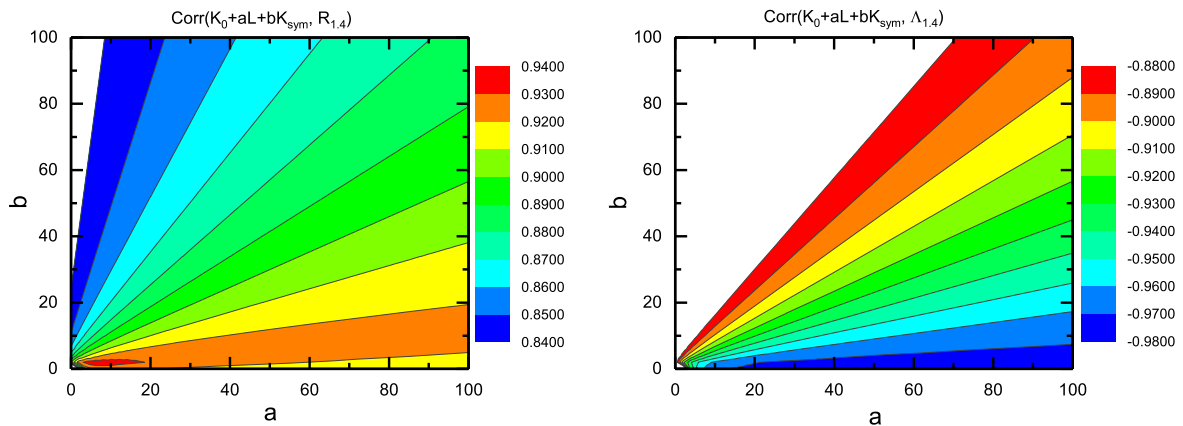


FIG. 5. The linear correlation coefficients between the linear combination of three NM parameters $K_0 + aL + bK_{\text{sym}}$ and global properties of NS at $1.4M_\odot$, where a, b are the combination coefficients, respectively. Left panel: correlations with the radius $R_{1.4}$; right panel: correlations with the dimensionless tidal deformability $\Lambda_{1.4}$.

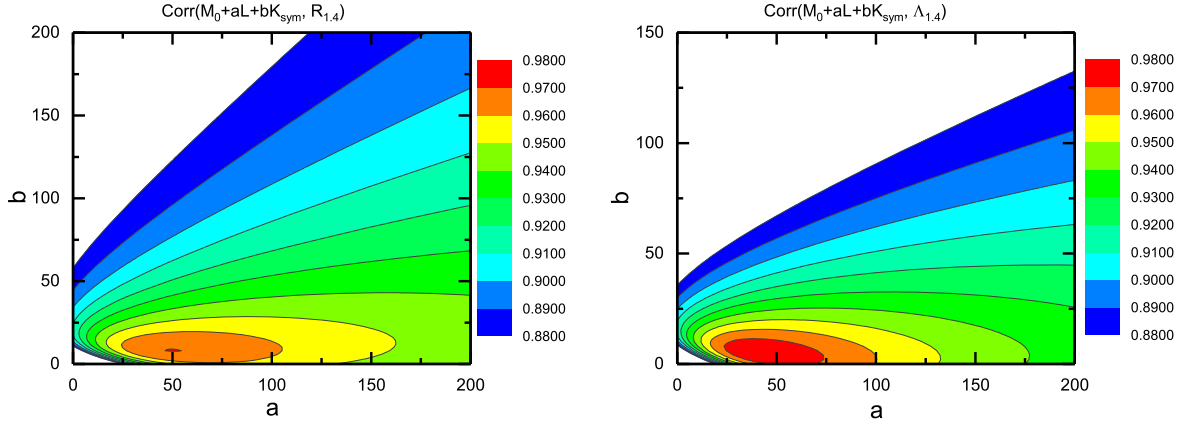


FIG. 6. Same as Fig. 5, but for the results of the linear combination of three NM parameters $M_0 + aL + bK_{\text{sym}}$.

All of the discussions in Sec. III are about the typical NSs, such as the $1.4M_\odot$ NS. Next we will focus on the low-mass neutron stars. Up to now, many astronomical observations have provided evidence for the existence of low-mass NSs [41–43]. So far, there have been many studies on the low-mass NSs [73–77]. For example, Sotani *et al.* especially studied the properties of low-mass NSs by defining a nonlinear combination of the NM parameters $\eta = (K_0 L^2)^{1/3}$ [73–75,77]. In this work, we will also concern the correlations between the properties of low-mass NSs and the NM parameters. Except for analyzing the correlation between the properties of low-mass NSs and the general NM parameters, we also introduce the results of η for comparison. Our calculation results show that only L and η have a good correlation with the low-mass NS properties, the results of other NM parameters are just poor. Figure 7 shows in detail the results of correlations

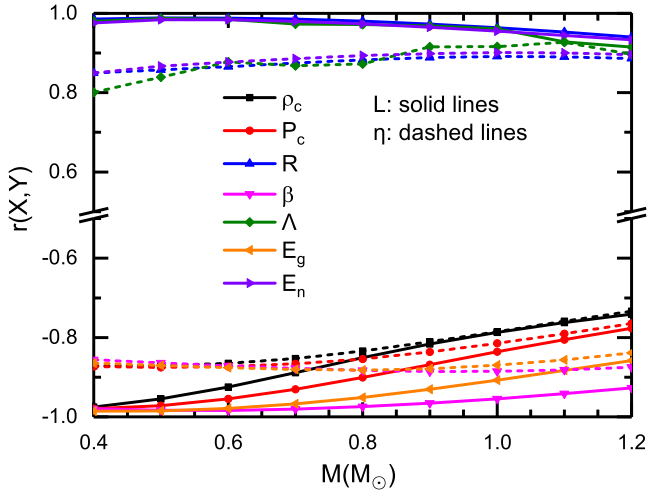


FIG. 7. The linear correlation coefficients $r(X, Y)$ between the slope of symmetry energy L or the parameter combination $\eta = (K_0 L^2)^{1/3}$ and the properties of low-mass NSs at fixed mass as functions of the NS mass $M(M_\odot)$. The solid and dashed lines represent the results of L and η , respectively.

between L (η) and different NS properties in the low mass region of NSs (0.4 – $1.2M_\odot$). It is found that L and η are well correlated with the properties of low-mass NSs. And L has a better correlation with the properties of low mass NSs than η . This shows that in addition to the parameter η , L can also be used to describe the properties of low mass NSs.

Using the constraint on $L = 54 \pm 8$ MeV from Ref. [22], we can constrain some observable properties of low-mass NSs and further compare them with the astronomical observations. Specifically, in this work, we analyzed the correlations between L and the gravitational binding energy $|E_g|$ of the low-mass NSs, which is shown in Fig. 8. The results clearly show that there exists a significant linear relation between L and $|E_g|$, which can be expressed as,

$$|E_{g,0.4}| = -3.653 \times 10^{-5} L + 0.019 = 0.017 M_\odot, \quad (3.10)$$

$$|E_{g,0.6}| = -7.864 \times 10^{-5} L + 0.041 = 0.036 - 0.037 M_\odot, \quad (3.11)$$

$$|E_{g,0.8}| = -1.311 \times 10^{-4} L + 0.072 = 0.064 - 0.066 M_\odot, \quad (3.12)$$

$$|E_{g,1.0}| = -1.968 \times 10^{-4} L + 0.112 = 0.100 - 0.103 M_\odot. \quad (3.13)$$

By using the constraint range of L , we can obtain the effective constraint on $|E_g|$ of the low-mass NSs. For example, for the $1.0M_\odot$ NSs, its $|E_g|$ is constrained in a range of 0.100 – $0.103M_\odot$. As the gravitational binding energy $|E_g|$ is associated with the total energy released from a supernova [36,78], it will be possible to predict whether the remainder is a low-mass NS by measuring the total released energy of a supernova in the future.

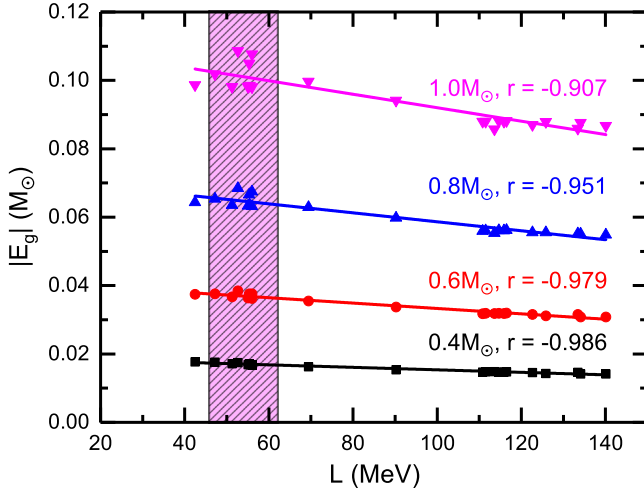


FIG. 8. The correlations between the slope of symmetry energy L and the gravitational binding energy $|E_g|$ of low-mass NSs at $M = 0.4, 0.6, 0.8, 1.0M_\odot$ respectively. The magenta shaded area represents the constraint on $L = 54 \pm 8$ MeV from Ref. [22].

IV. SUMMARY

At present, many properties of NSs have the obvious uncertainty, which requires us to adopt proper methods to constrain them. It is an effective method to constrain the NS properties by establishing the correlations between the NM parameters at saturation density and the relevant NS properties and combining with the specific constraints on NM parameters from the current terrestrial nuclear experiments. This can allow us not only to obtain effective constraints on the relevant properties of NSs, but also explore the relations between the NM physics and astronomical observations of NSs. In this work, we selected 22 sets of EOS based on the core-crust matching between the RMF and BPS + BBP models, systematically analyzed the correlations between the NM parameters and NS properties, and used the valid correlations found in this work to constrain the NS properties and compare them with the corresponding astronomical observations.

We first analyzed the correlations between a single NM parameter or a linear combination of two NM parameters and the NS properties. It is found that among all the above correlations, mainly R , Λ , β , E_n are well correlated with the slope of symmetry energy L . Further, we use the correlations of L and $M_0 + aL$ to constrain the $1.4M_\odot$ NS properties, such as the $R_{1.4}$ and $\Lambda_{1.4}$. It is found that the results of $R_{1.4}$ and $\Lambda_{1.4}$ restricted by the constraint $L = 54 \pm 8$ MeV based on the correlation $M_0 + aL$ are $R_{1.4} = 12.00\text{--}12.58$ km, $\Lambda_{1.4} = 321.7\text{--}561.3$, respectively, which can be well consistent with the constraint ranges of GW170817, NICER PSR J0030 + 0451, and other previous works. It is shown that the core-crust EOS matching has certain effect on the numerical results of the NS properties and their correlations with the NM parameters, but has little effect on the final qualitative conclusions.

Next, we extended the study on the influence of the linear or nonlinear combinations of NM parameters on the correlations. The results show that considering the linear combination of the third or more NM parameters has little effect on the correlation, so it needs no further consideration. Next, we analyzed the correlations between the properties of low-mass NSs and NM parameters. It is found that compared with the defined combination of the NM parameters $\eta = (K_0 L^2)^{1/3}$, there is a better correlation between L and the properties of low-mass NSs. As an application, we specifically use the correlation of $L\text{--}|E_g|$ to calculate $|E_g|$ of the low-mass NSs with the constraint on $L = 54 \pm 8$ MeV. For the $1.0M_\odot$ NSs, its $|E_g|$ is constrained in a range of $0.100\text{--}0.103M_\odot$. Therefore, the $|E_g|$ of low-mass NSs can be theoretically well constrained with the constraint range of L , which can be used to connect with the total energy released in a supernova and predict the formation of the low-mass NSs.

ACKNOWLEDGMENTS

This work is supported by NSFC (Grant No. 11975101), Guangdong Natural Science Foundation (Grants No. 2020A151501820 and No. 2022A1515011552).

-
- [1] J. M. Lattimer and M. Prakash, *Science* **304**, 536 (2004).
 - [2] B. P. Abbott *et al.*, *Phys. Rev. Lett.* **119**, 161101 (2017).
 - [3] B. P. Abbott *et al.*, *Astrophys. J. Lett.* **848**, L12 (2017).
 - [4] B. P. Abbott *et al.*, *Phys. Rev. Lett.* **121**, 161101 (2018).
 - [5] A. W. Steiner, M. Prakash, J. M. Lattimer, and P. J. Ellis, *Phys. Rep.* **411**, 325 (2005).
 - [6] J. M. Lattimer and M. Prakash, *Phys. Rep.* **621**, 127 (2016).
 - [7] M. Oertel, M. Hempel, T. Klöhn, and S. Typel, *Rev. Mod. Phys.* **89**, 015007 (2017).
 - [8] K. Yagi and N. Yunes, *Phys. Rep.* **681**, 1 (2017).
 - [9] B. A. Li, P. G. Krastev, D. H. Wen, and N. B. Zhang, *Eur. Phys. J. A* **55**, 117 (2019).
 - [10] A. W. Steiner, J. M. Lattimer, and E. F. Brown, *Astrophys. J.* **722**, 33 (2010).
 - [11] N. Alam, B. K. Agrawal, M. Fortin, H. Pais, C. Providência, Ad. R. Raduta, and A. Sulaksono, *Phys. Rev. C* **94**, 052801 (R) (2016).
 - [12] S. De, D. Finstad, J. M. Lattimer, D. A. Brown, E. Berger, and C. M. Biwer, *Phys. Rev. Lett.* **121**, 091102 (2018).

- [13] T. Malik, N. Alam, M. Fortin, C. Providência, B. K. Agrawal, T. K. Jha, B. Kumar, and S. K. Patra, *Phys. Rev. C* **98**, 035804 (2018).
- [14] J. L. Jiang, S. P. Tang, D. S. Shao, M. Z. Han, Y. J. Li, Y. Z. Wang, Z. P. Jin, Y. Z. Fan, and D. M. Wei, *Astrophys. J.* **885**, 39 (2019).
- [15] J. L. Jiang, S. P. Tang, Y. Z. Wang, Y. Z. Fan, and D. M. Wei, *Astrophys. J.* **892**, 55 (2020).
- [16] M. Ferreira, M. Fortin, T. Malik, B. K. Agrawal, and C. Providência, *Phys. Rev. D* **101**, 043021 (2020).
- [17] R. Essick, I. Tews, P. Landry, and A. Schwenk, *Phys. Rev. Lett.* **127**, 192701 (2021).
- [18] B. K. Agrawal, T. Malik, J. N. De, and S. K. Samaddar, *Eur. Phys. J. Special Topics* **230**, 517 (2021).
- [19] S. Huth *et al.*, *Nature (London)* **606**, 276 (2022).
- [20] D. Adhikari *et al.*, *Phys. Rev. Lett.* **126**, 172502 (2021).
- [21] B. T. Reed, F. J. Fattoyev, C. J. Horowitz, and J. Piekarewicz, *Phys. Rev. Lett.* **126**, 172503 (2021).
- [22] P. G. Reinhard, X. R. Maza, and W. Nazarewicz, *Phys. Rev. Lett.* **127**, 232501 (2021).
- [23] E. Annala, T. Gorda, A. Kurkela, and A. Vuorinen, *Phys. Rev. Lett.* **120**, 172703 (2018).
- [24] C. Y. Tsang, M. B. Tsang, P. Danielewicz, F. J. Fattoyev, and W. G. Lynch, *Phys. Lett. B* **796**, 1 (2019).
- [25] Y. Zhou, L. W. Chen, and Z. Zhang, *Phys. Rev. D* **99**, 121301(R) (2019).
- [26] O. Lourenço, M. Dutra, C. H. Lenzi, C. V. Flores, and D. P. Menezes, *Phys. Rev. C* **99**, 045202 (2019).
- [27] R. Nandi, P. Char, and S. Pal, *Phys. Rev. C* **99**, 052802(R) (2019).
- [28] I. Tews, J. Margueron, and S. Reddy, *Eur. Phys. J. A* **55**, 97 (2019).
- [29] L. Perot, N. Chamel, and A. Sourie, *Phys. Rev. C* **100**, 035801 (2019).
- [30] H. Tong, P. W. Zhao, and J. Meng, *Phys. Rev. C* **101**, 035802 (2020).
- [31] O. Lourenço, M. Dutra, C. H. Lenzi, S. K. Biswal, M. Bhuyan, and D. P. Menezes, *Eur. Phys. J. A* **56**, 32 (2020).
- [32] F. J. Fattoyev and J. Piekarewicz, *Phys. Rev. C* **86**, 015802 (2012).
- [33] T. Malik, B. K. Agrawal, J. N. De, S. K. Samaddar, C. Providência, C. Mondal, and T. K. Jha, *Phys. Rev. C* **99**, 052801(R) (2019).
- [34] T. Malik, B. K. Agrawal, C. Providência, and J. N. De, *Phys. Rev. C* **102**, 052801(R) (2020).
- [35] B. A. Li and A. W. Steiner, *Phys. Lett. B* **642**, 436 (2006).
- [36] R. R. Jiang, D. H. Wen, and H. Y. Chen, *Phys. Rev. D* **100**, 123010 (2019).
- [37] W. J. Sun, D. H. Wen, and J. Wang, *Phys. Rev. D* **102**, 023039 (2020).
- [38] S. Yang, D. H. Wen, J. Wang, and J. Zhang, *Phys. Rev. D* **105**, 063023 (2022).
- [39] J. D. Walecka, *Ann. Phys.* **83**, 491 (1974).
- [40] M. Dutra, O. Lourenço, S. S. Avancini, B. V. Carlson, A. Delfino, D. P. Menezes, C. Providência, S. Typel, and J. R. Stone, *Phys. Rev. C* **90**, 055203 (2014).
- [41] V. S. Petrov, E. A. Antokhina, and A. M. Cherepashchuk, *Astronomy Reports* **57**, 669 (2013).
- [42] M. L. Rawls, J. A. Orosz, J. E. McClintock, M. A. P. Torres, C. D. Bailyn, and M. M. Buxton, *Astrophys. J.* **730**, 25 (2011).
- [43] V. Suleimanov, J. Poutanen, M. Revnivtsev, and K. Werner, *Astrophys. J.* **742**, 122 (2011).
- [44] J. N. De, S. K. Samaddar, and B. K. Agrawal, *Phys. Rev. C* **92**, 014304 (2015).
- [45] M. Dutra, O. Lourenço, and D. P. Menezes, *Phys. Rev. C* **93**, 025806 (2016).
- [46] A. Sulaksono and T. Mart, *Phys. Rev. C* **74**, 045806 (2006).
- [47] F. J. Fattoyev, C. J. Horowitz, J. Piekarewicz, and G. Shen, *Phys. Rev. C* **82**, 055803 (2010).
- [48] T. Klähn *et al.*, *Phys. Rev. C* **74**, 035802 (2006).
- [49] S. Typel and H. H. Wolter, *Nucl. Phys. A* **656**, 331 (1999).
- [50] X. Roca-Maza, X. Viñas, M. Centelles, P. Ring, and P. Schuck, *Phys. Rev. C* **84**, 054309 (2011).
- [51] T. Nikšić, D. Vretenar, P. Finelli, and P. Ring, *Phys. Rev. C* **66**, 024306 (2002).
- [52] G. A. Lalazisis, T. Nikšić, D. Vretenar, and P. Ring, *Phys. Rev. C* **71**, 024312 (2005).
- [53] W. H. Long, J. Meng, N. V. Giai, and S. G. Zhou, *Phys. Rev. C* **69**, 034319 (2004).
- [54] B. Wei, Q. Zhao, Z. H. Wang, J. Geng, B. Y. Sun, Y. F. Niu, and W. H. Long, *Chin. Phys. C* **44**, 074107 (2020).
- [55] S. Typel, *Phys. Rev. C* **71**, 064301 (2005).
- [56] S. Typel, G. Röpke, T. Klähn, D. Blaschke, and H. H. Wolter, *Phys. Rev. C* **81**, 015803 (2010).
- [57] P. G. Reinhard, *Rep. Prog. Phys.* **52**, 439 (1989).
- [58] M. Bender, K. Rutz, P. G. Reinhard, J. A. Maruhn, and W. Greiner, *Phys. Rev. C* **60**, 034304 (1999).
- [59] G. Lalazisis, S. Karatzikos, R. Fossion, D. P. Arteaga, A. Afanasjev, and P. Ring, *Phys. Lett. B* **671**, 36 (2009).
- [60] G. A. Lalazisis, J. König, and P. Ring, *Phys. Rev. C* **55**, 540 (1997).
- [61] Y. Sugahara and H. Toki, *Nucl. Phys. A* **579**, 557 (1994).
- [62] M. M. Sharma, A. R. Farhan, and S. Mythili, *Phys. Rev. C* **61**, 054306 (2000).
- [63] G. Baym, C. J. Pethick, and P. Sutherland, *Astrophys. J.* **170**, 299 (1971).
- [64] G. Baym, H. A. Bethe, and C. J. Pethick, *Nucl. Phys. A* **175**, 225 (1971).
- [65] M. Fortin, C. Providência, Ad. R. Raduta, F. Gulminelli, J. L. Zdunik, P. Haensel, and M. Bejger, *Phys. Rev. C* **94**, 035804 (2016).
- [66] L. Suleiman, M. Fortin, J. L. Zdunik, and P. Haensel, *Phys. Rev. C* **104**, 015801 (2021).
- [67] J. R. Oppenheimer and G. M. Volkoff, *Phys. Rev.* **55**, 374 (1939).
- [68] R. C. Tolman, *Phys. Rev.* **55**, 364 (1939).
- [69] T. E. Riley *et al.*, *Astrophys. J. Lett.* **887**, L21 (2019).
- [70] M. C. Miller *et al.*, *Astrophys. J. Lett.* **887**, L24 (2019).
- [71] T. E. Riley *et al.*, *Astrophys. J. Lett.* **918**, L27 (2021).
- [72] M. C. Miller *et al.*, *Astrophys. J. Lett.* **918**, L28 (2021).
- [73] H. Sotani, K. Iida, K. Oyamatsu, and A. Ohnishi, *Prog. Theor. Exp. Phys.* **2014**, 051E01 (2014).
- [74] H. O. Silva, H. Sotani, and E. Berti, *Mon. Not. R. Astron. Soc.* **459**, 4378 (2016).
- [75] H. Sotani, *Phys. Rev. C* **95**, 025802 (2017).
- [76] Y. M. Wen and D. H. Wen, *Phys. Rev. C* **95**, 065804 (2017).
- [77] H. Sotani, *Phys. Rev. D* **102**, 063023 (2020).
- [78] B. Reed and C. J. Horowitz, *Phys. Rev. D* **102**, 103011 (2020).